Charras et al., http://www.jcb.org/cgi/content/full/jcb.200602085/DC1

Supplemental information

Constitutive expression of ezrin mutants modulates the proportion of blebbing cells

Stable cell lines expressing the FERM domain of ezrin-GFP, ezrin T567A-GFP, or ezrin T567D-GFP were derived from wild-type M2 cells. T567A impairs actin binding, but promotes association with the membrane where it can oligomerize with wild-type ezrin,

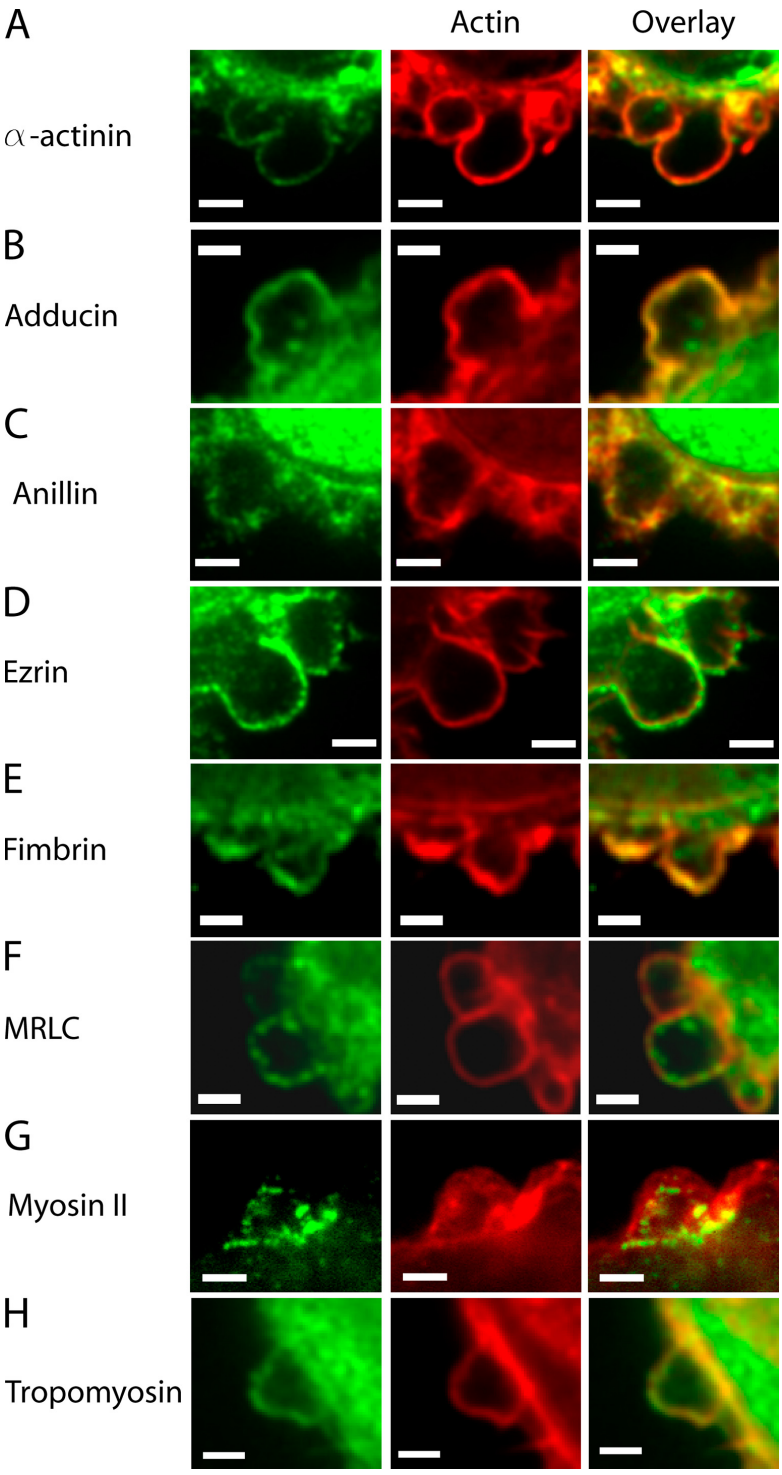

Figure S1. Protein localization in fixed blebbing cells using immunofluorescence. All images were acquired using confocal microscopy. α-Actinin (A), adducin (B), anillin (C), fimbrin (E), and tropomyosin (H) colocalized exactly with the new actin polymer. (D) Ezrin was displaced toward the cell exterior compared to the actin cortex. MRLC (F) and myosin II (G) assembled in distinct puncta and were displaced toward the cell interior compared to the actin cortex. Bars, 2 μm.

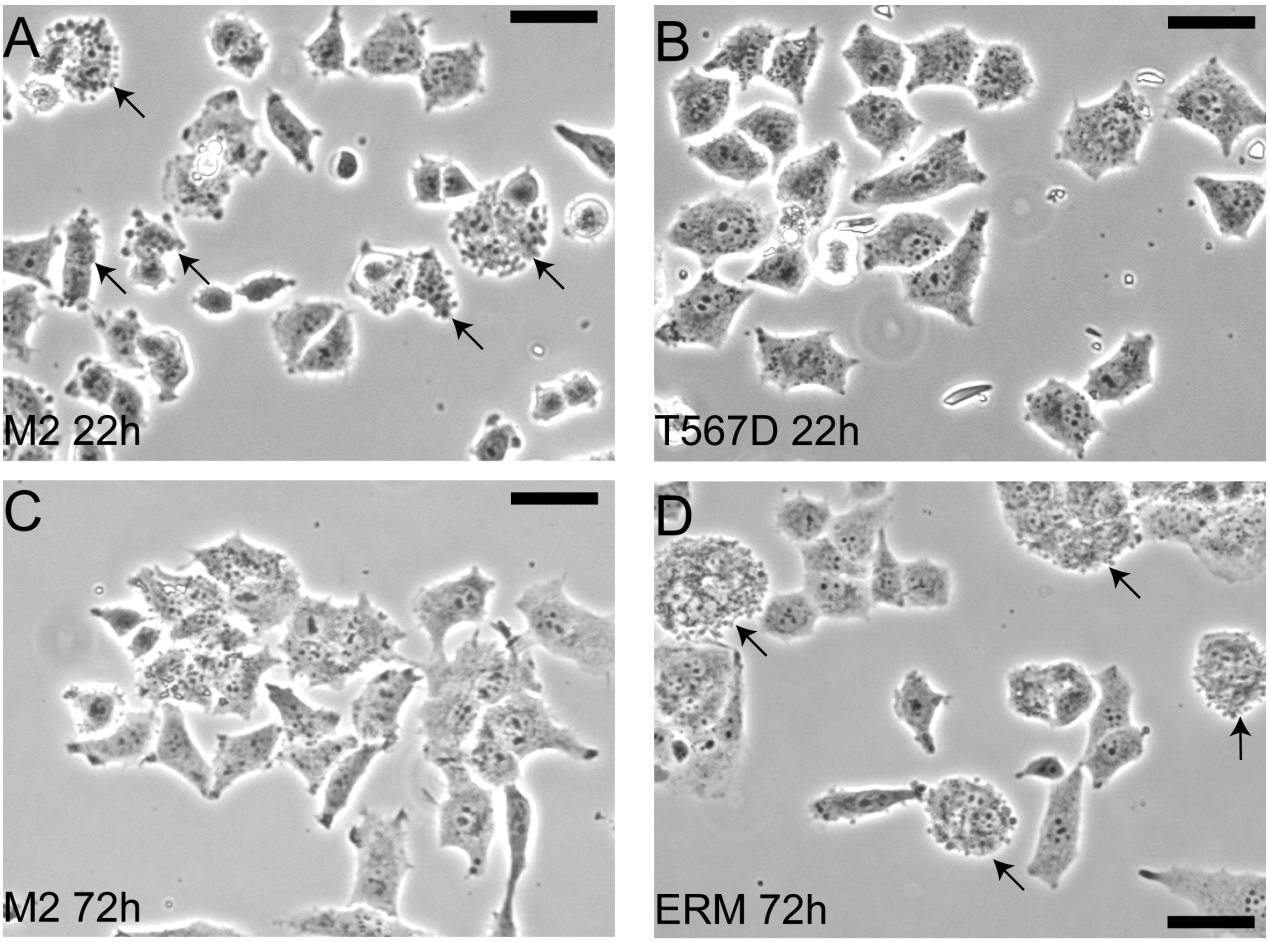

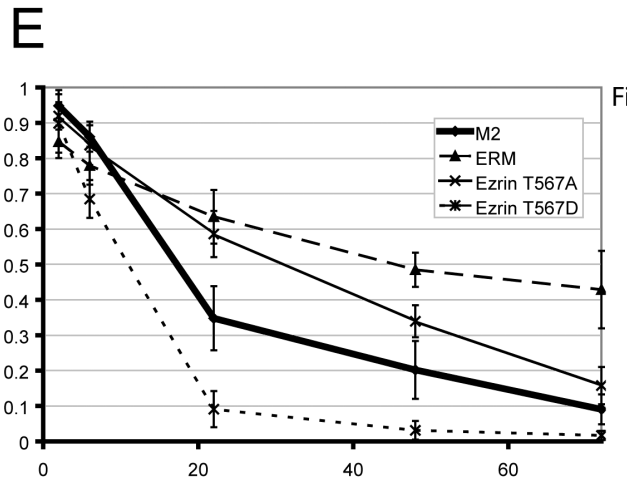

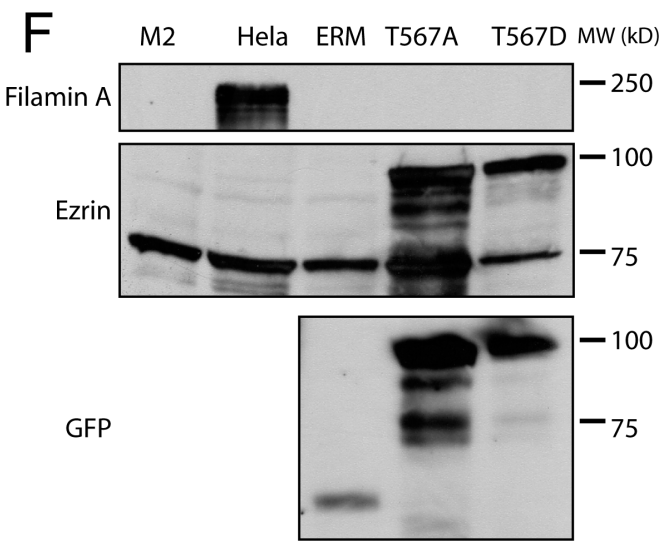

Figure S2. Ezrin stabilizes cell shape. All images were acquired with phase contrast with a 10× objective. (A) Wild-type M2 cells after 22 h of plating. Many cells exhibit blebs (arrows). (B) M2-ezrin T567D cells after 22 h of plating. Most cells are well spread and have an elongated shape. (C) Wild-type M2 cells after 72 h of plating. Most cells have spread. (D) M2-FERM cells after 72 h of plating. A large percentage of cells still bleb (arrows), are poorly spread, and grow in clumps. (E) Time course of the percentage of blebbing cells for wild-type cells, M2-ezrin T567D, M2-ezrin T567A, and M2-FERM cells. Error bars represent the SD. M2-ezrin T567D cells stop blebbing significantly faster than wild-type cells, whereas M2-ezrin T567A or M2-FERM cells stop blebbing significantly later. (F) Western blot of the different cell types showing the expression of filamin, ezrin, ezrin-GFP, and the FERM domain of ezrin-GFP. The cell lines to which each lane corresponds are indicated at the top. The antibodies used for blotting are indicated on the left, and the molecular weights are indicated on the right. None of the M2 cell lines express filamin. HeLa cells serve as a positive control for filamin expression. Stable expression of ezrin-GFP was detected in M2-ezrin T567A and T567D cells with both anti-ezrin and anti-GFP antibodies. When anti-ezrin antibodies are used, two bands shifted by the molecular weight of GFP are detected in the T567A and T567D cell lines in addition to wild-type ezrin. Stable expression of the FERM domain of ezrin-GFP was detected with anti-GFP antibodies. Bars, 50 μm.

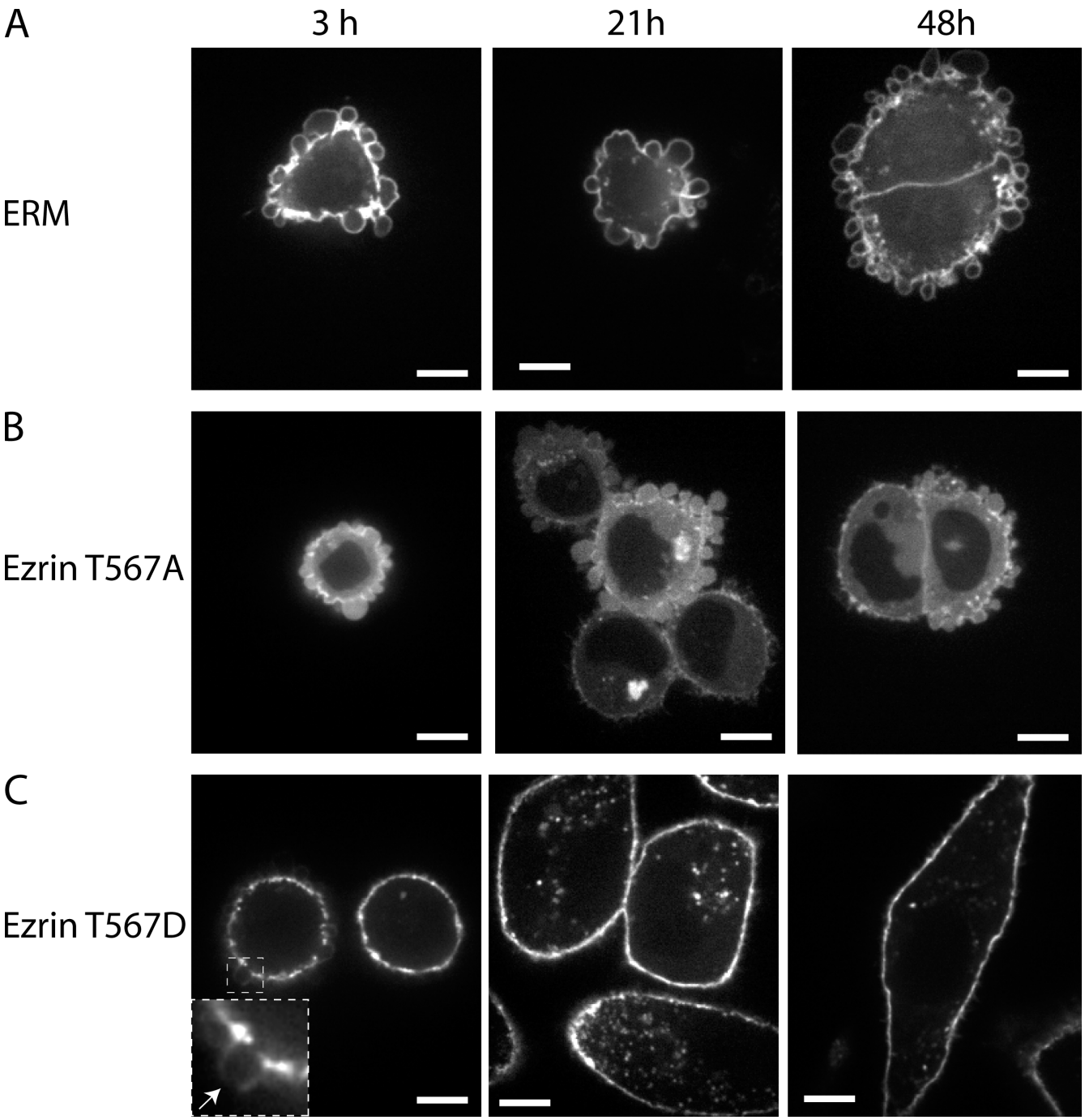

Figure S3. Localization of GFP-tagged ezrin mutants in spreading cells at different times after plating. All images were acquired using confocal microscopy. (A) At all time points, the FERM domain of ezrin-GFP localized to the cell membrane in both expanding and retracting blebs. (B) Ezrin T567A-GFP localizes to the cytoplasm, the cortex, and the membrane of retracting blebs at all time points. (C) Ezrin T567D-GFP is primarily located to the cortex of cells. After 3 h of plating, some cells still bleb, but ezrin T567D-GFP is primarily located to their cortex (inset). In cells that have spread for longer, all of ezrin T567D-GFP is localized to the cortex. Bars, 10 μm.

thereby acting as a dominant-negative protein, whereas T567D mimics phosphorylation and promotes association with the actin cytoskeleton, thereby acting as a dominant-active protein (Gautreau et al., 2000).

To create the stable cell lines, cells were transfected with the appropriate ezrin mutant, selected, and regrown from single clones. Protein expression and localization were checked by immunoblotting and fluorescence microscopy, respectively. In all cases, at least three cell lines showing similar characteristics were obtained. We confirmed by immunoblotting that none of the cell lines expressed filamin (Fig. S2 F; using HeLa cells as a positive control) and that they stably expressed the ezrin constructs at levels comparable to wild-type ezrin (Fig. S2 F).

Table S1. **Detailed information about all of the plasmids used in this study**

Protein	Accession number	Domain	Species	Source	Reference
β-Actin		full length	human	CLONTECH Laboratories, Inc.	
Adducin	BC013393	full length	human	Open Biosystems	This paper
α-Actinin	NM001102	full length	human	Open Biosystems	This paper
Anillin		full length	human	C. Field	Oegema et al., 2000
Ankyrin B		full length	rat	V. Bennett	Mohler et al., 2002
Annexin II	NM1002858	full length	human	M2 mRNA	This paper
Arp3		full length	human	D. Schafer	Welch et al., 1997
Capping protein		full length	human	D. Schafer	Schafer et al., 1998
Coronin-3	NM014325	full length	human	M2 mRNA	This paper
Ezrin	NM003379	full length	human	M2 mRNA	This paper
Ezrin		6xHis-FERM domain-mRFP	human	V. Gerke	Koltzscher and Gerke, 2000
Fascin		full length	mouse	P. McCrea	Tao et al., 1996
Fimbrin	NM005032	full length	human	M2 mRNA	This paper
KIAA0861	BC064632	full length	human	Open Biosystems	This paper
mDia1		full length	mouse	N. Watanabe	Watanabe et al., 1999
MHC	AF055895	full length	*X. laevis*	A. Straight	Straight et al., 2005
Moesin		full length	rat	H. Furthmayr	Amieva et al., 1999
mRFP		full length		R. Tsien	Shaner et al., 2004
MRLC	BC046702	full length	*X. laevis*	A. Straight	Straight et al., 2005
Myr2	NM023092	full length	rat	T. Lechler	
Myr3	NM173101	full length	rat	T. Lechler	
Net 1	BC053553	full length	human	Open Biosystems	This paper
P50RhoGAP	NM004308	catalytic fragment	human	A. Hall	
PLCδ	U09117	PH domain	human	T. Balla	Varnai and Balla, 1998
Protein 4.1	BC039079	full length	human	Open Biosystems	This paper
RhoA	NM001664	full length	human	A. Hall	
RhoGDIa	NM004309	full length	human	A. Hall	
Rhotekin		GTP-binding domain	human	W. Bement	Bement et al., 2005
Rhotekin		6xHis-GTP-binding domain-mRFP	human	R. Grosse	Goulimari et al., 2005
Septin 6		full length	human	M. Kinoshita	Kinoshita et al., 2002
TDRFP		full length		R. Tsien	Shaner et al., 2004
Tropomodulin 3	BC047163	full length	*X. laevis*	N. Watanabe	
Tropomyosin 4	BC057705	full length	*X. laevis*	N. Watanabe	
Tubulin alpha		full length	human	CLONTECH Laboratories, Inc.	
VASP	BC015289	full length	human	Open Biosystems	This paper
Vimentin		full length	human	R. Goldman	Yoon et al., 1998

M2 cells bleb profusely after plating, and the proportion of blebbing cells slowly decreases over a period of days (Cunningham, 1995). To test the effect of ezrin mutants on blebbing, we imaged the cell lines at different time points after plating and determined the proportion of blebbing cells. Fewer cells expressing ezrin T567D-GFP blebbed compared with wild type at all time points after 22 h ($P < 0.01$ in all cases; Fig. S2 E). Cells stably expressing ezrin T567A-GFP or the FERM domain of ezrin-GFP had a significantly higher proportion of blebbing cells than the wild type (Fig. S2, C–E) for time points ≥22 h. This trend subsisted throughout the examination period for the FERM domain of ezrin-GFP and until 48 h for ezrin T567A-GFP (Fig. S2 E).

Localization of the GFP-tagged mutant ERM proteins was examined by confocal microscopy (Fig. S3). Localization of wild-type ezrin was already discussed (Fig. 2, A and B; and Fig. 5A). At all time points, ezrin T567D-GFP was primarily concentrated at the bulk actin cortex. Fewer cells expressing this construct blebbed, but when they did, the ezrin mutant was largely excluded from the bleb membrane (Fig. S3 C, 3 h, inset). One of the most striking features of ezrin T567D-GFP cells is that even the cells that do not bleb undergo vigorous contractions. Ezrin T567A-GFP localized to the cytoplasm and to retracting blebs (Fig. S3 B) and its dynamics resembled that of wild-type ezrin. Unlike wild-type ezrin, the FERM domain of ezrin-GFP localized to the membrane only in both expanding and contracting blebs (Fig. S3 A).

References

Amieva, M.R., P. Litman, L. Huang, E. Ichimaru, and H. Furthmayr. 1999. Disruption of dynamic cell surface architecture of NIH3T3 fibroblasts by the N-terminal domains of moesin and ezrin: in vivo imaging with GFP fusion proteins. *J. Cell Sci.* 112:111–125.

Goulimari, P., T.M. Kitzing, H. Knieling, D.T. Brandt, S. Offermanns, and R. Grosse. 2005. Galpha12/13 is essential for directed cell migration and localized Rho-Dia1 function. *J. Biol. Chem.* 280:42242–42251.

Kinoshita, M., C.M. Field, M.L. Coughlin, A.F. Straight, and T.J. Mitchison. 2002. Self- and actin-templated assembly of Mammalian septins. *Dev. Cell.* 3:791–802.

Koltzscher, M., and V. Gerke. 2000. Identification of hydrophobic amino acid residues involved in the formation of S100P homodimers in vivo. *Biochemistry.* 39:9533–9539.

Mohler, P.J., A.O. Gramolini, and V. Bennett. 2002. The ankyrin-B C-terminal domain determines activity of ankyrin-B/G chimeras in rescue of abnormal inositol 1,4,5-trisphosphate and ryanodine receptor distribution in ankyrin-B (−/−) neonatal cardiomyocytes. *J. Biol. Chem.* 277:10599–10607.

Oegema, K., M.S. Savoian, T.J. Mitchison, and C.M. Field. 2000. Functional analysis of a human homologue of the *Drosophila* actin binding protein anillin suggests a role in cytokinesis. *J. Cell Biol.* 150:539–552.

Schafer, D.A., M.D. Welch, L.M. Machesky, P.C. Bridgman, S.M. Meyer, and J.A. Cooper. 1998. Visualization and molecular analysis of actin assembly in living cells. *J. Cell Biol.* 143:1919–1930.

Shaner, N.C., R.E. Campbell, P.A. Steinbach, B.N. Giepmans, A.E. Palmer, and R.Y. Tsien. 2004. Improved monomeric red, orange and yellow fluorescent proteins derived from Discosoma sp. red fluorescent protein. *Nat. Biotechnol.* 22:1567–1572.

Tao, Y.S., R.A. Edwards, B. Tubb, S. Wang, J. Bryan, and P.D. McCrea. 1996. β-Catenin associates with the actin-bundling protein fascin in a noncadherin complex. *J. Cell Biol.* 134:1271–1281.

Varnai, P., and T. Balla. 1998. Visualization of phosphoinositides that bind pleckstrin homology domains: calcium- and agonist-induced dynamic changes and relationship to myo-[^{3}H]inositol-labeled phosphoinositide pools. *J. Cell Biol.* 143:501–510.

Watanabe, N., T. Kato, A. Fujita, T. Ishizaki, and S. Narumiya. 1999. Cooperation between mDia1 and ROCK in Rho-induced actin reorganization. *Nat. Cell Biol.* 1:136–143.

Welch, M.D., A.H. DePace, S. Verma, A. Iwamatsu, and T.J. Mitchison. 1997. The human Arp2/3 complex is composed of evolutionarily conserved subunits and is localized to cellular regions of dynamic actin filament assembly. *J. Cell Biol.* 138:375–384.

Yoon, M., R.D. Moir, V. Prahlad, and R.D. Goldman. 1998. Motile properties of vimentin intermediate filament networks in living cells. *J. Cell Biol.* 143:147–157.